The second-generation exportin-1 inhibitor KPT-8602 demonstrates potent activity against acute lymphoblastic leukemia

Thomas Vercruysse[1*], Jolien De Bie[2,3*], Jasper E Neggers[1*], Maarten Jacquemyn[1], Els Vanstreels[1], Jonathan L Schmid-Burgk[4], Veit Hornung[4], Erkan Baloglu[5], Yosef Landesman[5], William Senapedis[5], Sharon Shacham[5], Antonis Dagklis[2,3], Jan Cools[2,3], Dirk Daelemans[1]

[1]KU Leuven Department of Immunology and Microbiology, Laboratory of Virology and Chemotherapy, Rega Institute for Medical Research, 3000 Leuven, Belgium

[2]KU Leuven Department of Human Genetics, Laboratory of Molecular Biology of Leukemia, 3000 Leuven, Belgium

[3]VIB Center for the Biology of Disease, 3000 Leuven, Belgium

[4]Institute of Molecular Medicine, University Hospital, University of Bonn, Sigmund-Freud-Str. 25, 53127 Bonn, Germany

[5]Karyopharm Therapeutics Inc, Newton, MA, 02459, USA

[*] *These authors contributed equally to this work*

Correspondence: Dirk Daelemans,
KU Leuven,
Rega Institute for Medical Research,
Minderbroedersstraat 10,
3000 Leuven, Belgium
dirk.daelemans@kuleuven.be

Running title: Anti-ALL activity of KPT-8602

Translational relevance

The paper describes the drug-target validation and acute lymphoblastic (ALL) activity of the second-generation XPO1 inhibitor KPT-8602, which has been introduced to human clinical trials in January 2016 to study its safety, tolerability and efficacy. KPT-8602 displays potent anti-leukemia activity both in ALL cell lines as well as in a mouse ALL model and in patient-derived xenograft T- and B-ALL models, supporting further clinical development of this drug for the treatment of ALL.

Abstract

Purpose: Human exportin-1 (XPO1) is the key nuclear-cytoplasmic transport protein that exports many cargo proteins out of the nucleus. Inducing nuclear accumulation of these proteins by inhibition of XPO1 causes cancer cell death. First clinical validation of pharmacological inhibition of XPO1 was obtained with the Selective Inhibitor of Nuclear Export (SINE) compound selinexor (KPT-330) demonstrating activity in Phase-II/IIb clinical trials when dosed 1 – 3 times weekly. The second-generation SINE compound KPT-8602 shows improved tolerability and can be dosed daily. Here we investigate and validate the drug-target interaction of KPT-8602 and explore its activity against acute lymphoblastic leukemia (ALL).

Experimental design: We examined the effect of KPT-8602 on XPO1 function and XPO1-cargo as well as on a panel of leukemia cell lines. Mutant XPO1 leukemia cells were designed to validate KPT-8602's drug-target interaction. *In vivo*, anti-ALL activity was measured in a mouse ALL model and patient-derived ALL xenograft models.

Results: KPT-8602 induced caspase-dependent apoptosis in a panel of leukemic cell lines *in vitro*. Using CRISPR/Cas9 genome editing we demonstrated the specificity of KPT-8602 for cysteine 528 in the cargo-binding groove of XPO1 and validated the drug target interaction. *In vivo*, KPT-8602 showed potent anti-leukemia activity in a mouse ALL model as well as in patient-derived T- and B-ALL xenograft models without affecting normal hematopoiesis.

Conclusions: KPT-8602 is highly specific for XPO1 inhibition and demonstrates potent anti-leukemic activity supporting clinical application of the second-generation SINE compound for the treatment of ALL.

Introduction

Exportin-1 (XPO1), also known as chromosome region maintenance 1 (CRM1), is the best-characterized nuclear transporter that mediates the export of a wide range of different proteins, including transcription factors, tumour suppressor proteins, and cell cycle regulators from the nucleus to the cytoplasm. In recent years, XPO1 overexpression has been observed in different types of cancer and is related to tumour size and patient outcome (1-6). In addition, a recurrent mutation in codon 571 of *XPO1* (p.E571K/G), located in the hydrophobic cargo-binding pocket has been reported in CLL (7) and AML (8).

XPO1 has been considered a desirable molecular target for cancer treatment for over 20 years and has resulted in several studies of diverse structurally unique small molecule inhibitors. Until recently, Leptomycin B (LMB) was the only compound that was investigated in the clinic. However, LMB was discontinued due to toxic side effects including nausea, gastrointestinal effects and fatigue (9). More recently, orally bioavailable small-molecule XPO1 inhibitors called Selective Inhibitors of Nuclear Export (SINE) compounds have been developed, with KPT-330 (Selinexor, Karyopharm Therapeutics) as the lead clinical compound. Selinexor is being investigated in multiple phase 1 and 2 clinical studies in various solid and hematological malignancies. In addition, SL-801 (Stemline Therapeutics) has recently been approved for clinical investigation in patients with advanced solid tumours. SINE compounds are optimized derivatives of the *N*-azolylacrylate class of small-molecule XPO1 inhibitors (10, 11), which prevent nuclear export of cargo proteins. At the molecular level these compounds covalently bind to the reactive cysteine residue at position 528 in the hydrophobic binding groove of XPO1 (12, 13)

Selinexor shows promising results as single agent in patients with heavily pre-treated relapsed/refractory haematological or solid cancers (14, 15) and is currently being evaluated in combination with other chemotherapeutic agents. As of today >1400 patients have been treated

with selinexor. While activity for selinexor is evident from these clinical trials, its dosing is limited to twice weekly to minimize any potential adverse events. It was hypothesized that increasing the reversibility of the covalent binding to XPO1 may increase tolerability. Therefore, KPT-8602 (**Fig. 1A**) was designed to bear a Michael acceptor activated with an additional electron withdrawing group at the Cα (16). KPT-8602 has reduced brain penetration (17) and displays improved tolerability as compared to selinexor allowing daily dosing. KPT-8602 has been introduced to human clinical trials in January 2016 to study its safety, tolerability and efficacy in patients with relapsed/refractory multiple myeloma (NCT02649790).

Here we validate the drug-target interaction for KPT-8602 and demonstrate potent inhibitory activity against various leukemia cell lines as well as strong *in vivo* activity for the treatment of acute lymphoblastic leukemia (ALL). ALL is a severe hematologic cancer with a peak incidence in young children. Although the overall survival is now >90% for childhood ALL, the outcome in infants, adults and relapse patients remains poor (18). In addition, treatment of ALL consists of toxic chemotherapeutic dosing schemes with severe long-term side effects (19), including the risk of developing a secondary malignancy (20). Newly discovered targeted therapies usually inhibit one specific genomic aberration, limiting treatment to only a small subset of patients. Compounds that target nuclear export, such as selinexor or KPT-8602, could potentially be used for the treatment of different ALL subtypes, independent of molecular characteristics.

Materials and Methods

Cell lines and reagents

T-ALL cells Jurkat, MOLT-4, ALL-SIL, DND41, and HPB-ALL; B-ALL cells BV173, EHEB, and REH; and myeloid leukaemia cells MV4-11, MOLM13, K-562, and HL-60 were acquired from ATCC or DSMZ and cultured in RPMI 1640 medium supplemented with 10% v/v fetal bovine serum and 20 µg/mL gentamicin. The haploid HAP-1 cells, derived from KBM-7 CML cells, (Horizon Discovery) were maintained in IMDM supplemented with 10 % fetal bovine serum and 20 µg/mL gentamicin. All cells lines were thawed upon receipt from the distributor, they were amplified and subsequently frozen in batches. After thawing of these lots, cell lines were kept no longer than 6 months in culture. Identity of leukemia cell lines was confirmed by karyotyping and full exome sequencing. Transfected HeLa NLS_{SV40}-AcGFP-NES_{PKI} were maintained in DMEM supplemented with 10% v/v FBS and 20 µg/mL gentamicin. Peripheral blood mononuclear cells (PBMCs) were isolated by density centrifugation (Lymphoprep). Cell viability was measured using a three day MTS assay (Promega), AlexaFluor488 Annexin V-Dead Cell Viability flow cytometry (Life Technologies), and/or the Acridine Orange (AO) / Propidium Iodide (PI) Cell Viability Kit (Westburg). CC_{50} values were calculated by fitting the obtained MTS cell viability data in GraphPad Prism using a 4-parameter log based fit for inhibitors.

XPO1 phenotypic reporter assay and colocalization with Rev-BFP

In order to study the XPO1-mediated nuclear export, a stably transfected HeLa SV40/NLS-AcGFP-NES/PKI reporter cell-line was used. In order to knock-out XPO1 protein expression by indel formation in the *XPO1* gene, cells were transfected with a plasmid expressing the Cas9 endonuclease N-terminally fused to the NLS of SV40 and the P2A-mCherry domain to visualize transfection, and a plasmid expressing a sgRNA targeting *XPO1* (target sequence 5'-GGATTATGTGAACAGAAAAG-3') using a Neon Transfection System (10 µL, 1475V, 10 ms, 3x, buffer R). Transfected and untransfected cells were then plated into an 8-well glass bottom µ-slide (IBIBI) containing DMEM. Two days later, the untransfected cells were treated with either DMSO or 1 µM KPT-8602 for 3 hours and then all

cells, including the XPO1 knockout cells, were visualized for AcGFP localization using confocal fluorescence microscopy.

For colocalization of Rev-BFP and XPO1-mNeonGreen, HAP-1 cells stably expressing XPO1 fused c-terminally to mNeonGreen were electroporated with a plasmid encoding for HIV-1 Rev-BFP using the Neon Transfection System (10 µL, 1475V, 10 ms, 3x, buffer R) and plated into an 8-well glass bottom µ-slide (IBIBI) containing IMDM. Cells were then imaged the next day and treated with either DMSO or 2 µM KPT-8602. After two hours of treatment, Rev-BFP and XPO1-mNeonGreen were visualized by confocal fluorescence microscopy.

Microscopy

Transfected HeLa cells were imaged with a Leica TCS SP5 confocal microscope (Leica Microsystems, Mannheim, Germany), employing a HCX PL APO 63x (NA 1.2) water immersion objective. Different fluorochromes were detected sequentially using excitation lines of 405 nm (BFP), 488 nm (AcGFP, mNeonGreen, YFP, Alexa Fluor 488). Emission was detected between 410-480 nm (BFP), 493-565 nm (AcGFP, mNeonGreen, Alexa Fluor 488), or 500-580 nm (YFP).

High content imaging and analysis

Stably transfected HeLa SV40/NLS-AcGFP-NES/PKI reporter cells seeded in a 96-well imaging plate (Falcon), were treated with different doses of compound or solvent (DMSO) for 4h. After treatment the cells were fixed and their nuclei counterstained with DAPI or Hoechst 33342. Fluorescence in the blue and green channel was read on an ArrayScan XTI High Content Reader (ThermoFisher Scientific). Nuclear and cytoplasmic compartments were segmented and their average pixel intensities were quantitated employing the HCS Studio software. GraphPad Prism software was used for calculation of EC_{50} values based on the relative change (as compared to the DMSO control) of the percentage nuclear AcGFP signal for the different treatments. Experiments were repeated six times on three different dates.

Immunofluorescence staining

For immunostaining of endogenous XPO1 in HAP-1 wild-type cells, cells were plated into a Labtek 8-well chambered cover glass, pretreated with 0.1% (w/v) poly-L-lysine (Sigma). Cells were allowed to adhere to the slides and were fixed in 4% paraformaldyhe (PFA) in PBS. Following fixation, cells were washed with PBS and then permeabilized using 0.2% Triton X-100 in PBS. After permeabilization, cells were washed and further immunofluorescence staining was performed according to standard procedure. Antibodies included the primary XPO1 antibody and a secondary Alexa Fluor 488 conjugated antibody. Stained cells were then analyzed by confocal fluorescence microscopy.

For the p53 staining, MOLT-4 cells were treated with 10 µM of compound or solvent (DMSO) for 3h. Cells were harvested, washed in PBS and then transferred into a Labtek 8-well chambered cover glass, pretreated with 0.1% (w/v) poly-L-lysine (Sigma). Cells were allowed to adhere to the slides and were then subsequently fixed (4% PFA in PBS), washed and permeabilized (0.2% Triton X-100 in PBS). Further immunofluorescence staining was then performed according to standard procedures. Employed antibodies included mouse monoclonal anti-p53 (DO-1) (sc-126, Santa Cruz Biotechnology) at a 1:100 dilution and secondary Alexa Fluor® 488 goat anti-mouse antibody (A11001, Molecular Probes). Cell nuclei were counterstained with DAPI and the samples were imaged by confocal microscopy. The fluorescence in the green channel was quantitated on a per cell basis employing CellProfiler image analysis software, nuclei were segmented based on the DAPI staining and the cytoplasm was defined by expanding the nuclei by a distance of N=6 pixels. A total of ~200 cells were analyzed for each condition. For each cell the ratio of the mean pixel intensities in nucleus vs. cytoplasm was calculated, as well as the mean pixel intensity of the entire cell. Results were analyzed using a two-sided unpaired t-test with Welch's correction (**** $p<0.0001$ or *** $p<0.0005$) and are depicted as mean +/- 95% CI.

CRISPR/Cas9 knock-in

CRISPR/Cas9 genome editing of HL-60, Jurkat, K-562, and MOLT-4 cell lines was performed as described in (13). Briefly, cells were transfected with plasmids expressing Cas9-NLS_{SV40}, single guide RNA (target sequence 5'-GGATTATGTGAACAGAAAAG-3') targeting *XPO1* and the ssDNA donor oligonucleotide (IDT) containing the Cys528Ser missense mutation. Following electroporation with a Neon Electroporation system (ThermoFisher) (10 µL, 1350V, 10 ms, 3x, buffer R), cells were plated in 1 mL prewarmed, antibiotic free RPMI 1640 medium supplemented with 10% v/v FBS. After two days the medium was refreshed and KPT-185 was added to a final concentration of 100 nM-1 µM, depending on cell line. After 1-2 weeks, surviving cells were diluted in 96-wells to obtain single colonies (0.5 cell/well). Following cell growth, confluent 96-wells containing the single colonies were washed and then lysed in Bradley lysis buffer (10 mM Tris-HCl (pH 7.5), 10 mM EDTA, 0.5% SDS, 10 mM NaCl and 1 µg/mL proteinase K) for two hours at 56°C. The genomic DNA was extracted from the lysates using ethanol/salt precipitation coupled to centrifugation. The target site, the DNA sequence around *XPO1*, was amplified by PCR with the following primers: fwd: 5'-TCTGCCTCTCCGTTGCTTTC, rv: 5'-CCAATCATGTACCCCACAGCT. After PCR, the products were sequenced by Sanger Sequencing (Macrogen) using a forward and reverse primer (5'-TGTGTTGGGCAATAGGCTCC, 5'-GGCATTTTTGGGCTATTTTAATGAAA respectively).

For knock-in of the Glu571Lys/Gly missense mutation, HAP-1 cells (Horizon Discovery) were transfected with Cas9-NLS_{SV40} together with a plasmid encoding a sgRNA targeting *XPO1* at Glu571 (5'-AAGCTGTTCGAATTCATGCA-3') and a donor repair template ssDNA oligonucleotide (IDT) carrying the desired mutation (Glu571G or K) and 1 additional silent mutation: (5'-GGTCAATACCCACGTTTTTTGAGAGCTCACTGGAAATTTCTGAAGACTGTAGTTAACAAGCTGTTC**GGA**TT**t**ATGCATGGTAAATCTCTTTCTTTACTATATTTTGCTTTTATTTTTATTGAAGAAAATAAATGAATGTTTTTGTCT-3'

and 5'-GGTCAATACCCACGTTTTTTGAGAGCTCACTGGAAATTTCTGAAGACTGTAGTTAACAAGCTGTTC**AAA**TT**t**ATGCATGGTAAATCTCTTTCTTTACTATATTTTGCTTTTATTTTTATTGAAGAAAATAAATGAATGTTTTTGTCT-3' respectively). Cells were electroporated using the Neon Electroporation system

(ThermoFisher) (10 µL, 1475V, 10 ms, 3x, buffer R) and plated immediately in 1 mL prewarmed, antibiotic free IMDM medium supplemented with 10% v/v FBS. Five days after transfection, cells were diluted (0.5 cell/well) into 96-well plates and scored for the formation of single colonies after 3 days. Single colonies were grown for a period of 2 weeks and the DNA was extracted as described above. The initial PCR and Sanger Sequencing was performed with the same primers as described above for the Cys528Ser knock-in.

For C-terminal knock-in of *mNeonGreen* into *XPO1*, the Cas9-NLS_{SV40} was again transfected together with a sgRNA targeting *XPO1* in the C-terminal region, just before the stop codon (target sequence: 5'-TTTTAATCACACATTTCTTC-3'). HAP-1 wild-type or $XPO1^{C528S}$ cells were electroporated using the same settings as described above and an additional donor repair plasmid containing the sequence for mNeonGreen-T2A-PuroR was added in order to facilitate insertion of *mNeonGreen* C-terminally to *XPO1* (21). Two days after electroporation, cells were selected for 5 days with 1 µg/mL puromycin and surviving cells were screened for the expression of XPO1-mNeonGreen. As almost all of the surviving cells showed green fluorescence with a typical pattern reminiscent of the endogenous XPO1 distribution, the polyclonal mixture was used for further experiments.

XPO1 Pull down and competition assay

For the initial pulldown of XPO1 with biotinylated KPT-8602 (KPT-9511), 10 million wild-type or $XPO1^{C528S}$ Jurkat cells were incubated at 37°C with 1 µM of KPT-9511 or DMSO in 1 mL of RPMI medium supplemented with 10% v/v FBS for two hours. Following incubation, cells were washed in ice-cold PBS and then lysed 20 minutes on ice in RIPA buffer (R0278, Sigma-Aldrich) supplemented with 1x HALT protease inhibitors (ThermoFisher). After lysis, the debris was collected by centrifugation (10 min., 20.000 x *g* at 4°C). A fraction was taken for the total lysate and the rest of the lysates were allowed to bind to Dynabeads MyOne Streptavidin T1 (Life Technologies) by rotating overnight at 4°C. The supernatant was removed the following morning and the beads were extensively washed in modified RIPA buffer (50 mM Tris-HCl [pH 7.8], 150 mM NaCl, 1% NP-40

[IGEPAL CA-630], 0.1% sodium deoxycholate, 1 mM EDTA) using a magnetic separator. Finally the bead-bound proteins were eluted for 10 minutes at 95°C with 1% SDS containing sample buffer (Protein Simple). Total protein concentrations were determined by the BCA assay (Thermo Scientific) and the samples were then prepared for Simple Western analysis according to protocol.

The competition experiment resembles a modified XPO1 pull down experiment. For this experiment, 5 million wild-type Jurkat cells were incubated for two hours with different concentrations of KPT-330 or KPT-8602 or DMSO in 0.5 mL of RPMI supplemented with 10% v/v FBS. Following this initial incubation period, 1 µM of the irreversible and biotinylated XPO1 inhibitor, KPT-9058, was added to the medium and incubated for 16 hours (overnight). In addition to KPT-9058, 10 µM of the pan caspase inhibitor Q-VD-OPh (Sigma-Aldrich) was also added to prevent apoptosis induction, together with 10 nM of bortezomib to prevent the proteasomal degradation of XPO1 proteins bound to the XPO1 inhibitors. The following morning cells were gathered and lysed for 15 minutes on ice in RIPA buffer supplemented with 1x HALT protease inhibitors. Afterwards the protein lysates were treated and XPO1 was extracted as described above for the initial XPO1 pull-down experiment.

Simple Western

Protein quantification and visualization was performed by Simple Western size-based protein assay (WES, ProteinSimple, Santa Clara, CA) a non-gel based and Westernblot-like substitute following manufacturer's protocol. For PARP and XPO1 protein quantification, cells were seeded at 0.,5 x 10^6 cells/ml in RPMI with 10% FBS. Compounds were added and incubated for 0-16h, washed with ice-cold phosphate buffered saline (PBS) and lysed in RIPA buffer (Cat no: R0278, Sigma) and 1x HALT protease inhibitor cocktail (Thermo Scientific) for 15 minutes on ice. Lysates were cleared by centrifugation and total protein concentrations were determined by BCA assay (Thermo Scientific). Protein lysates (~1-2 µg per lane) were loaded into each capillary and proteins of interest were identified using specific primary antibodies raised against PARP (#9542, Cell Signaling; 1:100), CRM1/XPO1 (NB100-79802, Novus; 1:12500), phospho-p53(Ser15) (#9284, Cell Signaling; 1:50) and

β-Tubulin (NB600-936, Novus; 1:3000) and probed with HRP conjugated secondary antibodies against mouse or rabbit (ProteinSimple). Chemiluminescence signals were exported from the Compass software (ProteinSimple).

***In vivo* drug formulation**

KPT-8602 (Karyopharm Therapeutics inc.) was formulated in 0.5% methylcellulose plus 1% Tween-80 and given by daily oral gavage at a concentration of 10-15 mg/kg. Placebo consisted of vehicle without KPT-8602.

Bone marrow transplantation assay

We transduced lineage negative mouse bone marrow cells with retroviral vectors containing cDNA of the JAK3 M511I mutant (Degryse et al., 2014). Transduced cells were injected into 4 irradiated BALB/c female mice of 6-8 weeks old. Blood samples were drawn every 2 weeks and measured with the Vet ABC^{TM} Hematology Analyzer (SCIL), while transduced cells were tracked by their expression of GFP+/mCherry+ on the MACSQuant VYB (Miltenyi Biotec). Treatment was initiated when white blood cell counts exceeded 10 000/µL, with > 50% mCherry+ leukemic cells.

Treatment of normal BALB/c mice

Five female BALB/c mice were randomly divided into 2 groups, with 3 animals receiving KPT-8602 and 2 animals receiving placebo. Mice were bled every week to determine the effect of treatment on all hematopoietic cell lines. Samples were analyzed with the Vet ABC^{TM} Hematology Analyzer (SCIL).

Patient derived xenograft models

Human leukemic bone marrow cells from NOTCH1 mutant T-ALL patient 389E and BCR-ABL1 positive B-ALL patient XC51 were injected into the tail vein of 6-to-12-week old NOD.Cg-*Prkdc*^{scid} *Il2rg*^{tm1Wjl}/SzJ (NSG) mice. After successful engraftment, splenocytes were harvested and reinjected at a

concentration of 1-2 x10^6 cells into 30 NSG-mice to create secondary transplants. Blood samples were taken once a week and measured on the Vet ABC ^{TM}Hematology Analyzer (SCIL). Leukemic engraftment was determined with flow cytometry (FACS Canto II, BD) using anti-human CD45 (APC, eBioscience) as marker for the leukemic cells.

Treatment started when the CD45-percentage in the peripheral blood was respectively <0.5% and >5%. Mice were divided into groups of 4-5 mice, each treated animal matching a control mouse in both gender and CD45%. At the end of treatment, mice were sacrificed and spleen and bone marrow harvested for single cell isolation and histopathologic examination. All experiments were conducted on protocols approved by the ethical committee of the University of Leuven.

Immunohistochemistry

Spleen tissue and sternum were collected and fixed in 10% neutral buffered formalin (Sigma) for 24 hours and then processed for paraffin embedding (Thermo Scientific ExcelsiorTM AS Tissue Processor and HistoStarTM Embedding Workstation). Sections of 5 µm were mounted on SuperfrostTM Plus Adhesion slides (Thermo Scientific) and stained with hematoxylin and eosin (Diapath). The degree of splenic or bone marrow colonization by leukemic cells was determined by staining with human HLA-A (Abcam) with a digital image analysis algorithm created on the ImageJ software platform.

Results

KPT-8602 inhibits XPO1-mediated nuclear cargo export

To assess the effect of KPT-8602 on XPO1 mediated nuclear export, it was tested in a phenotypic reporter assay of a GFP reporter protein that is fused to the NES from the cAMP-dependent protein kinase inhibitor (PKI) and to the SV40 NLS, which cause the GFP reporter to actively shuttle between nucleus and cytoplasm. In steady state the GFP fusion protein is mainly localized to the cytoplasm in a XPO1-dependent manner as knock out of XPO1 resulted in accumulation in the nucleus due to decreased nuclear export (**Fig. 1B**). HeLa cells stably expressing this GFP reporter protein were treated with increasing concentrations of KPT-8602 and the localization of GFP was determined by imaging (**Fig. 1C** and Supplementary Fig. S1). KPT-8602 inhibited the XPO1 dependent nuclear export with an EC_{50} value of 60.9 ± 3.6 nM, which is similar to the EC_{50} values for first-generation XPO1 inhibitor selinexor (55.7 ± 6.5 nM). Nuclear accumulation of the GFP reporter was observed as early as 4 minutes after treatment with 1 µM KPT-8602 (Supplementary movie S1). To investigate whether KPT-8602 effectively blocks the interaction of XPO1 with cargo protein in cells, we tagged cellular XPO1 protein with mNeonGreen in the genome of HAP-1 cells using CRISPaint gene tagging (21). The XPO1-mNeonGreen fusion protein was found at the nuclear membrane and throughout the nucleoplasm in agreement with the localization of untagged protein (**Fig. 1D**). When these cells were transfected with a plasmid expressing a Rev-BFP fusion, a prototype XPO1 cargo protein, a substantial fraction of the endogenous XPO1-mNeonGreen protein was co-localized with Rev-BFP in the nucleoli as a result of interaction between both proteins. Upon treatment of the cells with 2 µM KPT-8602 the Rev-dependent nucleolar co-localization was abolished demonstrating that KPT-8602 is effectively inhibiting the XPO1-cargo interaction (**Fig. 1E** and Supplementary movie S2). In addition, KPT-8602 also caused significantly decreased levels of XPO1 protein after overnight treatment, which was prevented by the proteasome inhibitor bortezomib suggesting a proteolytic degradation mechanism (**Fig. 1F**).

KPT-8602 directly binds XPO1

To further prove that KPT-8602 is inhibiting the XPO1-mediated nuclear export by directly targeting XPO1 we applied CRISPR/Cas9 genome editing to introduce a resistance Cys528Ser mutation in the *XPO1* gene of Jurkat leukemia cells (**Fig. 2A**) (13). The effect of the mutation on KPT-8602 activity was assessed by the visualization of the subcellular localization of the RanBP1 cargo (**Fig. 2B**). In both wild-type and mutant Jurkat cells RanBP1 localized in the cytoplasm. Upon treatment of wild-type cells with KPT-8602, RanBP1 accumulated in the nucleus. In contrast, KPT-8602 was unable to induce nuclear accumulation of the RanBP1 cargo in the XPO1^{C528S} mutant Jurkat cells, demonstrating that the mutation confers resistance to KPT-8602. This is supported by the observation that KPT-8602 was unable to inhibit the interaction between XPO1^{C528S} with its prototypical cargo protein, Rev (**Fig. 2C**).

To further demonstrate the direct binding of KPT-8602 to the XPO1 cysteine 528 residue, Jurkat cells were treated with biotinylated KPT-8602 (KPT-9511) (**Fig. 2D**) to pull down the compound from the lysate using streptavidin. KPT-9511 was able to pull down XPO1 protein from wild-type Jurkat cells, but not from Jurkat cells containing the homozygous XPO1^{C528S} mutation (**Fig. 2E, F**). To investigate whether the binding of KPT-8602 to XPO1 has increased reversibility as compared to selinexor, we used these compounds in a competition assay with a biotinylated analogue of KPT-276 (KPT-9058), which can also covalently interact with cys528 of XPO1 and can pull down XPO1 from cell lysates (13). When cells were pre-treated with selinexor, no binding of KPT-276 was detected, as the covalent binding of selinexor to XPO1 prevented the binding of KPT-9058 (**Fig. 2G**) (13, 22). If the interaction of KPT-8602 with XPO1 had increased reversibility compared to selinexor, KPT-9058 would outcompete KPT-8602 more efficiently than selinexor, resulting in increased amount of XPO1 being pulled down in the assay. However, at similar compound concentrations we did not observe a significant difference in the amount of pulled down XPO1 between KPT-8602 and selinexor treated cells.

KPT-8602 induces cytotoxicity and apoptosis in leukemia cell lines

To evaluate the anti-leukemic activity of KPT-8602, several human leukemia cell lines (T-ALL, B-ALL and AML) were cultured in the presence of increasing concentrations of KPT-8602 and cell viability was assessed after 72 hrs of treatment (**Fig. 3A**). Cell viability was reduced in all KPT-8602-treated leukemia cell lines with EC_{50} values ranging from 25 to 145 nM (Supplementary Table 1). Decrease in leukemia cell viability was further confirmed by annexin V/PI staining of Jurkat and MOLT-4 T-ALL cells (**Fig. 3B**). Both cell lines demonstrated pronounced levels of apoptosis measured 16 hrs after treatment. Induction of apoptosis was prevented by the pan-caspase inhibitor Q-VD-OPh, suggesting a caspase dependent mechanism. This was confirmed by the appearance of cleaved caspase-3 substrate PARP as early as 6 hours after treatment with 1 µM KPT-8602 (**Fig. 3C**). Normal PBMCs were unaffected up to 10 µM KPT-8602 (**Fig. 3D**).

Since the pro-apoptotic protein p53 is an important cargo of XPO1, we investigated if p53 localization was affected by KPT-8602 treatment. Treatment of MOLT-4 cells with KPT-8602 resulted in an increased p53 nuclear as well as absolute staining (**Fig 3E**). Upregulation and stabilisation of p53 in MOLT-4 (p53 wild-type as measured by exome seq) and BV173 (p53 wild-type (23)) was also evident by western blotting of phosphorylated (Ser15) p53 as early as 5 hours post treatment (**Fig 3F**). This correlated with the observed induction of apoptosis evident from the caspase dependent cleavage of PARP as early as 6 hours after treatment (**Fig 3C**).

Cytotoxic effects of KPT-8602 are completely attributed to XPO1 inhibition

To determine if the observed anti-leukemic activity of KPT-8602 was caused by its inhibition of XPO1 and not by off-target effects we tested the activity of KPT-8602 on 4 leukemia cell lines (Jurkat, MOLT-4, HL-60 and K562) in which we engineered the $XPO1^{C528S}$ mutant by CRISPR/Cas9 genome editing (**Fig. 3G**). For Jurkat, HL-60 and K562 we were able to select monoclonal homozygous mutants and for MOLT-4 we used the polyclonal cells. Mutant leukemia cells containing the single $XPO1^{C528S}$

mutation were 60-150 times more resistant to KPT-8602 than the parental cells (**Fig. 3H** and Supplementary Table 2), demonstrating that the C528S mutation confers resistance to the drug. This was confirmed by the absence of PARP cleavage in mutant Jurkat and MOLT-4 cells in the presence of micromolar concentrations KPT-8602 (**Fig. 3I**) and by the absence of decreased XPO1 protein levels (**Fig. 3J**). Altogether these results demonstrate that XPO1 is the target for KPT-8602 and that its anti-leukemic activity is completely caused by inhibition of XPO1-mediated nuclear protein export.

The XPO1 E571K/G mutation does not influence KPT-8602 activity

A recurrent mutation at codon 571 (p.E571K/G) in the *XPO1* gene was recently described in some leukemia patients (7, 8). Since this mutation is located inside the hydrophobic cargo-binding pocket near residue cysteine 528 of XPO1, we evaluated whether or not this mutation could affect KPT-8602 activity. Therefore we edited the *XPO1* gene of HAP-1 cells (CML) using CRISPR/Cas9 to introduce the E571K mutation and sensitivity of the mutant cells to KPT-8602 treatment was measured and compared to wild-type cells (**Fig 4**). The dose-dependent inhibitory curves of wild-type and mutant cells were identical for selinexor while KPT-8602 showed a different inhibitory curve for the mutant cells as compared to the wild-type suggesting a slightly increased activity towards the mutant.

KPT-8602 shows potent anti-lymphoblastic leukemia activity *in vivo*

To test the *in vivo* efficacy of KPT-8602, we first used the MOLT-4 T-ALL cell line in a subcutaneous murine xenograft model, which demonstrated potent anti-leukemia activity at daily doses between 5 and 15 mg/kg (**Fig. 5A**). Next, we used a mouse bone marrow transplant T-ALL model with the JAK3 (M511I) mutation, as previously described (24). Mice developed T-ALL after 100 to 200 days, characterized by elevated white blood cell (WBC) counts (>10 000 cells/µL) in the peripheral blood (PB). Mice received KPT-8602 at a dose of 15 mg/kg or placebo by daily oral gavage for 12 days and PB samples were taken at day 2 and at the end of the treatment period. After 2 days of treatment, animals already showed a marked reduction in total WBC counts compared to placebo-treated

animals and the WBC counts continued to drop until they reached normal levels (<10 000 cells/μL) by day 12 (**Fig. 5B**). This decrease in WBC was mostly due to loss of leukemic lymphocytes, however, a minor decrease in normal granulocyte numbers was also observed (**Fig. 5B**). To further investigate the effect of KPT-8602 on normal hematopoietic cells, we treated healthy Balb/c mice with KPT-8602 for 14 days, showing no or minimal changes in the normal blood cells or platelets during treatment (**Fig. 5C**).

KPT-8602 prolongs survival of patient derived xenograft models of ALL

To determine the activity of KPT-8602 against primary human leukemic cells, we next used a patient derived xenograft (PDX) model of a NOTCH1 mutant T-ALL sample and a BCR-ABL1 positive B-ALL sample with an IKZF1 deletion. Treatment consisted of KPT-8602 10 mg/kg or placebo once a day and was initiated when human leukemia cells in the PB of the mice ranged from 0 - 0.5%. After 3 to 4 weeks of treatment, all mice were sacrificed and their spleen, tibia and femur harvested for single cell isolation and histopathologic examination. Total WBC count of placebo- and drug-treated animals remained normal during treatment, as did the red blood cell and platelet counts, indicating that KPT-8602 treatment did not cause major effects on normal hematopoiesis (Supplementary Fig S2). However, mice that received KPT-8602 had significantly lower numbers of human leukemia cells in their PB, bone marrow (BM) and spleen, indicating that KPT-8602 treatment inhibited the growth of the human ALL cells (**Fig. 6A,B,G,H,J**). In addition, spleen weights at sacrifice in KPT-8602-treated animals were lower when compared to placebo-treated animals (**Fig. 6C,I**). Histopathologic examination confirmed the reduced organ infiltration of the leukemia cells in treated animals compared to placebo treated mice (**Fig. 6D**).

Since leukemia patients usually present with high WBC counts and severe organ invasion, we also tested the efficacy of KPT-8602 treatment in xenograft animals with high leukemic cell burden. Using the T-ALL PDX-model, we waited until mice had minimum 5% human leukemia cells in their PB

before starting treatment. To determine the survival benefit, mice were sacrificed when 50% or more human leukemia cells were detected in the PB, or if they fulfilled other ethical endpoint criteria. By the end of the third week, 4 out of 5 treated animals were still alive, compared to none of the placebo treated animals ($p = 0.0041$) (**Fig. 6E**). KPT-8602 was able to reduce the number of human leukemic cells in some animals, while stabilizing the disease in other animals (**Fig. 6F**).

Discussion

Acute lymphoblastic leukemia (ALL) is the most common childhood cancer. Although survival rates are high (>90%) with current treatment protocols, subgroups of patients still face unfavourable outcome, including infants, adults and relapse patients (18). In addition, survivors of ALL are often confronted with severe side effects of chemotherapy both on the short and long term. Especially in children, cardiomyopathy and osteopenia are well known consequences of chemotherapeutic regimens, while all treated patients face the risk of developing secondary malignancies (20). As new targeted therapies become available for specific subgroups of patients these will help to improve outcome and reduce toxic side effects. However, targeted inhibitors are typically very specific and can only be used for the treatment of a small number of patients, making both drug development and clinical evaluation of efficacy difficult. A more general targeted approach such as proteasome and now XPO1 inhibitors can overcome patient specificity problems and are likely to be effective for all leukemia subtypes, regardless of mutational status.

The lead clinical SINE compound, selinexor, is now in phase II/IIb clinical trials for several solid and hematological tumours. However selinexor dosing is restricted to 2-3 times per week due to adverse effects; primarily nausea, anorexia and fatigue (25). Here we tested a second-generation clinical stage SINE compound, KPT-8602, with improved tolerability allowing for daily dosing. We demonstrate that KPT-8602 is a potent XPO1 inhibitor with similar potency to selinexor *in vitro*. EC_{50} values were much below mean plasma concentrations reached (3 µM) in primates orally dosed at 10

mg/kg (17). KPT-8602 binds directly to XPO1, inhibits cargo interaction and subsequent cargo protein export from the nucleus resulting in nuclear accumulation of tumour suppressors. Indeed, KPT-8602 treatment caused nuclear accumulation of the tumour suppressor p53 resulting in caspase-dependent apoptosis induction. Introducing a serine mutation at cysteine 528 in multiple leukemia cell lines conferred drug resistance, thoroughly validating the drug-target interaction for KPT-8602. This cysteine mutation was experimentally identified as resistance mutation and has not been monitored in ongoing clinical trials. Although this cysteine is highly conserved amongst higher eukaryotes, mutations of this residue should be monitored as a mechanism for resistance in patients.

In vivo experiments showed potent anti-leukemic activity of KPT-8602 in both a mouse T-ALL model and two PDX ALL models, consistent with results from selinexor in preclinical and clinical phase I trials in patients with relapsed or refractory ALL and AML (NCT02091245). We did not observe evidence for toxic side effects of KPT-8602 dosed on a daily base at a concentration of 10 mg/kg. KPT-8602 had no effect on normal platelet, granulocyte or red blood cell counts in the PB of treated animals. This is important since decreases in normal hematopoietic cell numbers can lead to transfusion dependency or failed immune responses. As with selinexor, KPT-8602 may spare normal hematopoietic stem and progenitor cells (26). When treatment was started early on in ALL development, KPT-8602 was able to completely inhibit human leukemic cell growth in two PDX-models. However, to mimic the clinical situation of patients at diagnosis or relapse, we also set up a survival experiment starting therapy at a more advanced leukemic stage. As single agent, KPT-8602 was still able to reduce the leukemia cell numbers in 2 out of 5 mice, and stabilized the disease in the remaining animals. These findings together with its novel mode of action supports further investigation of KPT-8602 for the treatment of ALL in combination with standard therapy. Especially the observation that KPT-8602 shows potent activity against BCR-ABL1 positive ALL, which is a poor prognostic subtype of B-cell ALL, warrants further investigation of KPT-8602 for the treatment of such poor prognostic subgroups.

In conclusion, our data validate the second generation SINE compound KPT-8602 as a potent XPO1 inhibitor that can effectively inhibit leukemia growth *in vivo* with minimal effect on normal hematopoiesis.

Acknowledgements

We thank Lotte Bral, Bob Massant and Astrid D'Hoore for excellent technical help. This work was supported by grants from Kom op Tegen Kanker (J.C.), Stichting Tegen Kanker (J.C.), the European Research Council (J.C.) and the IAP network (J.C.). Part of this research work was performed using the 'Caps-It' research infrastructure (project ZW13-02) financially supported by the Hercules Foundation and Rega Foundation, KU Leuven; J.D.B. is supported by FWO-Vlaanderen, A.D. is supported by Kom op Tegen Kanker.

Conflicts of interest

EB, YL, WS, and SS are employees of Karyopharm Therapeutics. DD has a license agreement on SINE XPO1 inhibitors, the rest of the authors declare no conflicts of interest.

References

1. Huang WY, Yue L, Qiu WS, Wang LW, Zhou XH, Sun YJ. Prognostic value of CRM1 in pancreas cancer. Clin Invest Med 2009;32:E315.

2. Noske A, Weichert W, Niesporek S, Roske A, Buckendahl AC, Koch I, et al. Expression of the nuclear export protein chromosomal region maintenance/exportin 1/Xpo1 is a prognostic factor in human ovarian cancer. Cancer 2008;112:1733-43.

3. Shen A, Wang Y, Zhao Y, Zou L, Sun L, Cheng C. Expression of CRM1 in human gliomas and its significance in p27 expression and clinical prognosis. Neurosurgery. 2009;65:153-9.

4. van der Watt PJ, Maske CP, Hendricks DT, Parker MI, Denny L, Govender D, et al. The Karyopherin proteins, Crm1 and Karyopherin beta1, are overexpressed in cervical cancer and are critical for cancer cell survival and proliferation. Int J Cancer 2009;124:1829-40.

5. Yao Y, Dong Y, Lin F, Zhao H, Shen Z, Chen P, et al. The expression of CRM1 is associated with prognosis in human osteosarcoma. Oncol Rep. 2009;21:229-35.

6. van der Watt PJ, Zemanay W, Govender D, Hendricks DT, Parker MI, Leaner VD. Elevated expression of the nuclear export protein, Crm1 (exportin 1), associates with human oesophageal squamous cell carcinoma. Oncol Rep 2014;32:730-8.

7. Puente XS, Pinyol M, Quesada V, Conde L, Ordonez GR, Villamor N, et al. Whole-genome sequencing identifies recurrent mutations in chronic lymphocytic leukaemia. Nature. 2011;475:101-5.

8. Luthra R, Patel KP, Reddy NG, Haghshenas V, Routbort MJ, Harmon MA, et al. Next-generation sequencing-based multigene mutational screening for acute myeloid leukemia using MiSeq: applicability for diagnostics and disease monitoring. Haematologica. 2014;99:465-73.

9. Newlands ES, Rustin GJ, Brampton MH. Phase I trial of elactocin. Br J Cancer. 1996;74:648-9.

10. Daelemans D, Afonina E, Nilsson J, Werner G, Kjems J, De Clercq E, et al. A synthetic HIV-1 Rev inhibitor interfering with the CRM1-mediated nuclear export. Proc Natl Acad Sci U S A 2002;99:14440-5.

11. Van Neck T, Pannecouque C, Vanstreels E, Stevens M, Dehaen W, Daelemans D. Inhibition of the CRM1-mediated nucleocytoplasmic transport by N-azolylacrylates: structure-activity relationship and mechanism of action. Bioorg Med Chem 2008;16:9487-97.

12. Lapalombella R, Sun Q, Williams K, Tangeman L, Jha S, Zhong Y, et al. Selective inhibitors of nuclear export show that CRM1/XPO1 is a target in chronic lymphocytic leukemia. Blood 2012;120:4621-34.

13. Neggers JE, Vercruysse T, Jacquemyn M, Vanstreels E, Baloglu E, Shacham S, et al. Identifying drug-target selectivity of small-molecule CRM1/XPO1 inhibitors by CRISPR/Cas9 genome editing. Chem Biol. 2015;22:107-16.

14. Chen C, Gutierrez M, de Nully Brown P, Gabrail N, Baz R, Flinn I, et al. Anti-Tumor Activity of SELINEXOR (KPT-330), an Oral Selective Inhibitor of Nuclear Export (SINE), ± Dexamethasone in Multiple Myeloma Preclinical Models and Translation in Patients with Multiple Myeloma. EHA Annual Meeting 2014.

15. Kuruvilla J, Gutierrez M, Shah BD, Gabrail NY, de Nully Brown P, Stone RM, et al. Preliminary Evidence Of Anti Tumor Activity Of Selinexor (KPT-330) In a Phase I Trial Ofa First-In-Class Oral Selective Inhibitor Of Nuclear Export (SINE) In Patients (pts) With Relapsed / Refractory Non Hodgkin's Lymphoma (NHL) and Chronic Lymphocytic Leukemia (CLL). ASH Annual Meeting; New Orleans LA2013.

16. Serafimova IM, Pufall MA, Krishnan S, Duda K, Cohen MS, Maglathlin RL, et al. Reversible targeting of noncatalytic cysteines with chemically tuned electrophiles. Nat Chem Biol. 2012;8:471-6.

17. Hing ZA, Fung HYJ, Ranganathan P, Mitchell S, El-Gamal D, Woyach JA, et al. Next generation XPO1 inhibitor shows improved efficacy and in vivo tolerability in hematologic malignancies. Leukemia. 2016 In press

18. Inaba H, Greaves M, Mullighan CG. Acute lymphoblastic leukaemia. Lancet 2013;381:1943-55.

19. Te Winkel ML, Pieters R, Wind EJ, Bessems JH, van den Heuvel-Eibrink MM. Management and treatment of osteonecrosis in children and adolescents with acute lymphoblastic leukemia. Haematologica. 2014;99:430-6.

20. Robison LL, Bhatia S. Late-effects among survivors of leukaemia and lymphoma during childhood and adolescence. Br J Haematol. 2003;122:345-59.

21. Schmid-Burgk JL, Honing K, Ebert TS, Hornung V. CRISPaint allows modular base-specific gene tagging using a ligase-4-dependent mechanism. Nat Commun. 2016;7:12338.

22. Crochiere ML, Baloglu E, Klebanov B, Donovan S, Del Alamo D, Lee M, et al. A method for quantification of exportin-1 (XPO1) occupancy by Selective Inhibitor of Nuclear Export (SINE) compounds. Oncotarget. 2016;7:1863-77.

23. Peterson LF, Mitrikeska E, Giannola D, Lui Y, Sun H, Bixby D, et al. p53 stabilization induces apoptosis in chronic myeloid leukemia blast crisis cells. Leukemia 2011;25:761-9.

24. Degryse S, de Bock CE, Cox L, Demeyer S, Gielen O, Mentens N, et al. JAK3 mutants transform hematopoietic cells through JAK1 activation, causing T-cell acute lymphoblastic leukemia in a mouse model. Blood. 2014;124:3092-100.

25. Abdul Razak AR, Mau-Soerensen M, Gabrail NY, Gerecitano JF, Shields AF, Unger TJ, et al. First-in-Class, First-in-Human Phase I Study of Selinexor, a Selective Inhibitor of Nuclear Export, in Patients With Advanced Solid Tumors. J Clin Oncol 2016 In press

26. Etchin J, Sun Q, Kentsis A, Farmer A, Zhang ZC, Sanda T, et al. Antileukemic activity of nuclear export inhibitors that spare normal hematopoietic cells. Leukemia 2013;27:66-74.

Figure legends

Figure 1. KPT-8602 inhibits XPO1

A. Chemical structure of KPT-8602

B. XPO1 reporter assay. Confocal fluorescence microscopy of HeLa cells stably expressing the NLS-GFP-NES^{PKI} reporter after CRISPR/Cas9 knock-out of XPO1, or treatment with 1 μM KPT-8602

C. Quantification of increase in nuclear GFP signal of HeLa NLS-GFP-NES^{PKI} cells treated with different concentrations of selinexor (KPT-330) and KPT-8602. For each concentration a minimal number of 400 cells were analyzed. Data are presented as mean ± SD

D. Confocal fluorescence microscopy of HeLa cells immunostained for XPO1 (left) and of CRISPR/Cas9-induced tagged HAP-1$_{endo}$XPO1-mNeonGreen cells (right)

E. Confocal fluorescence microscopy of HAP-1$_{endo}$XPO1-mNeonGreen cells expressing Rev-BFP two hours after treatment with DMSO or 2 μM KPT-8602

F. Simple western for XPO1 of Jurkat cells treated with KPT-330 or KPT-8602 in the absence or presence of bortezomib. For each condition the ratio of XPO1/ β tubulin levels was quantified and normalized to untreated control. Data are presented as mean ± SD (n=2)

Figure 2 – Drug-target validation

A. Sequence chromatogram of genomic DNA from CRISPR/Cas9 genome edited Jurkat cells. Upper case indicate mutated bases, underlined bases are missense mutations and other upper case bases are silent mutations, italic cases indicate the PAM site

B. Confocal immunofluorescence imaging of RanBP1 cargo protein in wild-type and mutant Jurkat^{C528S} cells

C. Confocal fluorescence microscopy of HeLa cells co-expressing Rev-BFP and mutant XPO1^{C528S}-YFP 2 hours after treatment with DMSO or 2 μM KPT-8602

D. Chemical structure of biotinylated KPT-8602 (KPT-9511)

E. Pull-down of KPT-9511-bound XPO1 protein from Jurkat cells. Cells were incubated with DMSO or 1 μM KPT-9511 for 3 hr and streptavidin affinity chromatography was used to pull down XPO1 protein out of wild-type or mutant XPO1^{C528S} Jurkat cells

F. Quantification of pulled down XPO1 protein

G. KPT-330 and KPT-8602 bind to equal amounts of XPO1 in cells. Wild-type Jurkat cells were treated with either KPT-330 or KPT-8602 at different concentrations for 2 hours and subsequently incubated overnight with the biotinylated KPT-9058. Streptavidin affinity chromatography was used to pull down KPT-9058-bound XPO1 and analysed by simple western. The ratio of pulled down XPO1 over XPO1 input was quantified and normalized to untreated control (n=2). Data are presented as mean ± SD (n = 2).

Figure 3 - KPT-8602 induces potent cytotoxicity in T-ALL and B-cell leukemia cell lines

A. Viability of T-ALL, B-cell and AML leukemia cell lines treated with different concentrations KPT-330 or KPT-8602 as measured by MTS assay (n>=2). Data are presented as mean ± SD (n=3).

B. Cell viability as measured as measured by annexin V/PI staining flow cytometry at 16 hrs post treatment Data are presented as mean ± SD (n=3).

C. Lysates from Jurkat and MOLT-4 T-ALL, and BV173 B-ALL cells treated with 1 μM KPT-8602 were assessed for cleavage of PARP by simple western. *Lysate from cells treated with 1 μM KPT-8602 in the presence of the pancaspase inhibitor Q-VD-OPh

D. Viability of normal PBMC treated with KPT-330 and KPT-8602 as measured annexinV/PI flow cytometry and acridine orange/PI cell viability counting Data are presented as mean ± SD (n>=2).

E. Immunostaining of p53 in MOLT-4 cells treated with DMSO, 10 μM KPT-330 or 10 μM KPT-8602 for 3hrs. For each condition a total of ~200 cells were analyzed. For each cell the ratio of the mean pixel intensities in nucleus vs cytoplasm was calculated, as well as the mean

pixel intensity of the entire cell. Results were analyzed using a two-sided unpaired t-test with Welch's correction (**** p<0.0001 or *** p<0.0005) and are depicted as mean +/- 95% CI

F. Simple western for phospho-p53(Ser15) in MOLT-4 and BV173 whole cell extracts treated with 1 μM KPT-8602 for different times

G. Sequence chromatogram of genomic DNA from CRISPR/Cas9 genome edited leukemia cells. Upper case indicate mutated bases, underlined bases are missense mutations and other upper case bases are silent mutations, italic cases indicate the PAM site

H. Viability of wild-type and mutant XPO1^{C528S} leukemia cell lines treated with different concentrations KPT-330 and KPT-8602 as measured by MTS assay (n=3) Data are presented as mean ± SD (n=3)

I. Lysates from treated mutant XPO1^{C528S} Jurkat and MOLT-4 cells assessed for cleavage of PARP by simple western at different KPT-8602 concentrations and time points after treatment

J. Simple western for XPO1 levels and β tubulin of mutant XPO1^{C528S} Jurkat cells treated with KPT-330 or KPT-8602. For each condition the ratio of XPO1 over β tubulin levels was quantified and normalized to untreated control Data are presented as mean ± SD (n=2)

Figure 4 - KPT-8602 induces p53

Viability of CRISPR/Cas9 genome edited HAP-1 cells containing the E571K or G missense mutation treated with KPT-330 or KPT-8602 Data are presented as mean ± SD (n=3)

Figure 5 - KPT-8602 shows potent anti-lymphoblastic leukemia activity *in vivo*

A. MOLT-4 subcutaneous xenografted mice were treated with vehicle (n=8), doxorubicin at 5 mg/kg IP on days 1 and 15 (n=8), or KPT-8602 given PO at 5 (n=8) or 15 mg/kg (n=8) daily

B. Total white blood cell counts and absolute lymphocyte and granulocyte count in the peripheral blood of a mouse bone marrow transplant JAK3(M511I) T-ALL model, placebo (n=2) versus KPT-8602 (n=2) treated animals

C. Total white blood cell, lymphocyte, granulocyte, red blood cell (rbc) and platelet counts in wild-type BALB/c mice, treated for 14 days with KPT-8602 (n= 3) versus Placebo (n= 2)

Data information: in A-C data are presented as mean ± SD, ns: not significant

Figure 6 - KPT-8602 shows potent activity in patient derived ALL xenograft models.

A. Percentage of human leukemia cells (human CD45-positive cells) in the blood of mice injected with human T-ALL cells during treatment with placebo or KPT-8602. Start of the treatment is indicated (arrow)
B. Percentage of human leukemia cells (human CD45-positive cells) infiltrated in the bone marrow at the time of sacrifice in placebo versus KPT-8602 treated T-ALL PDX-animals
C. Comparison of spleen weights in KPT-8602 versus placebo treated T-ALL PDX-mice at the time of sacrifice
D. Human HLA-staining of spleen slides taken at sacrifice from a representative placebo-treated T-ALL PDX-mouse and KPT-8602-treated animal. (brown = infiltrating human leukemia cells, blue = normal mouse spleen tissue)
E. Survival analysis of 5 KPT-8602 and 5 Placebo treated T-ALL PDX-mice. Treatment started at day 28 after injection, when the percentage of human leukemia cells (human CD45-positive cells) in the blood > 5%. Animals were sacrificed when they reached ethical endpoints or the percentage human CD45-positive cells in the blood was 50% or more
F. Percentage of human leukemia cells (human CD45-positive cells) in the blood of mice injected with human T-ALL cells during treatment with placebo or KPT-8602. Treatment started when human CD45% in the blood reached > 5% (indicated with arrow). *There are no error bars at day 39 in the placebo treated group since at this time point the last remaining placebo mouse was sacrificed

G. Percentage of human leukemia cells (human CD45-positive cells) in the blood of mice injected with human BCR-ABL1 positive B-ALL cells during treatment with placebo or KPT-8602. Start of the treatment is indicated (arrow)

H. Percentage of human leukemia cells (human CD45-positive cells) infiltrated in the bone marrow at the time of sacrifice in placebo versus KPT-8602 treated B-ALL PDX-animals.

I. Comparison of spleen weights in KPT-8602 versus placebo treated B-ALL PDX-mice at the time of sacrifice

J. Percentage of human leukemia cells (human CD45-positive cells) infiltrated in the spleen tissue at the time of sacrifice in placebo versus KPT-8602 treated B-ALL PDX-animals.

Data information: in A-C and F-J data are presented as mean ± SD, p-values are calculated using Mann-Whitney U test

FIGURE 1

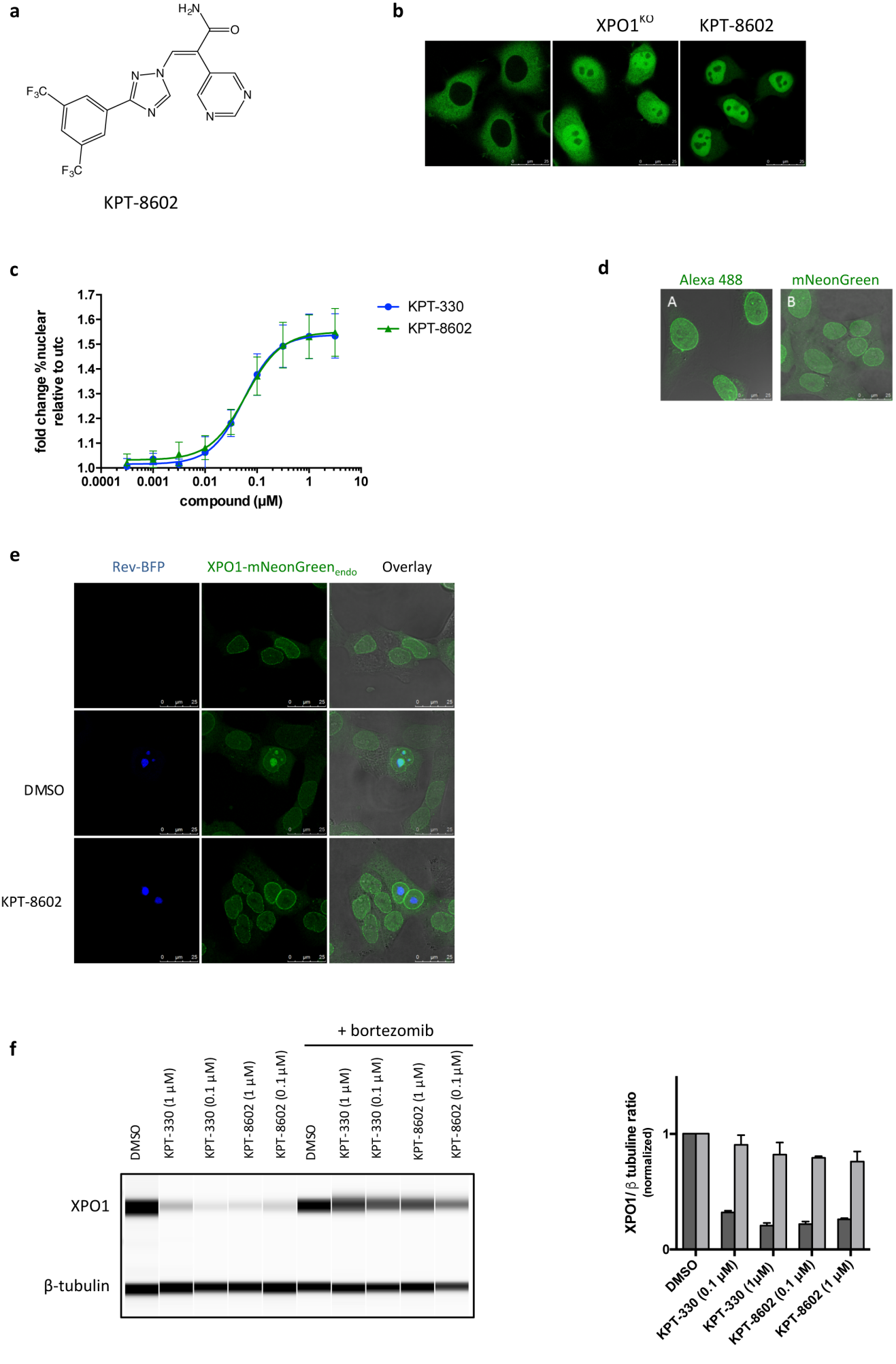
a
KPT-8602
b
XPO1KO
KPT-8602
c
fold change %nuclear relative to utc
compound (μM)
KPT-330
KPT-8602
d
Alexa 488
mNeonGreen
A
B
e
Rev-BFP
XPO1-mNeonGreenendo
Overlay
DMSO
KPT-8602
f
+ bortezomib
DMSO
KPT-330 (1 μM)
KPT-330 (0.1 μM)
KPT-8602 (1 μM)
KPT-8602 (0.1 μM)
XPO1
β-tubulin
XPO1/β tubuline ratio (normalized)

FIGURE 2

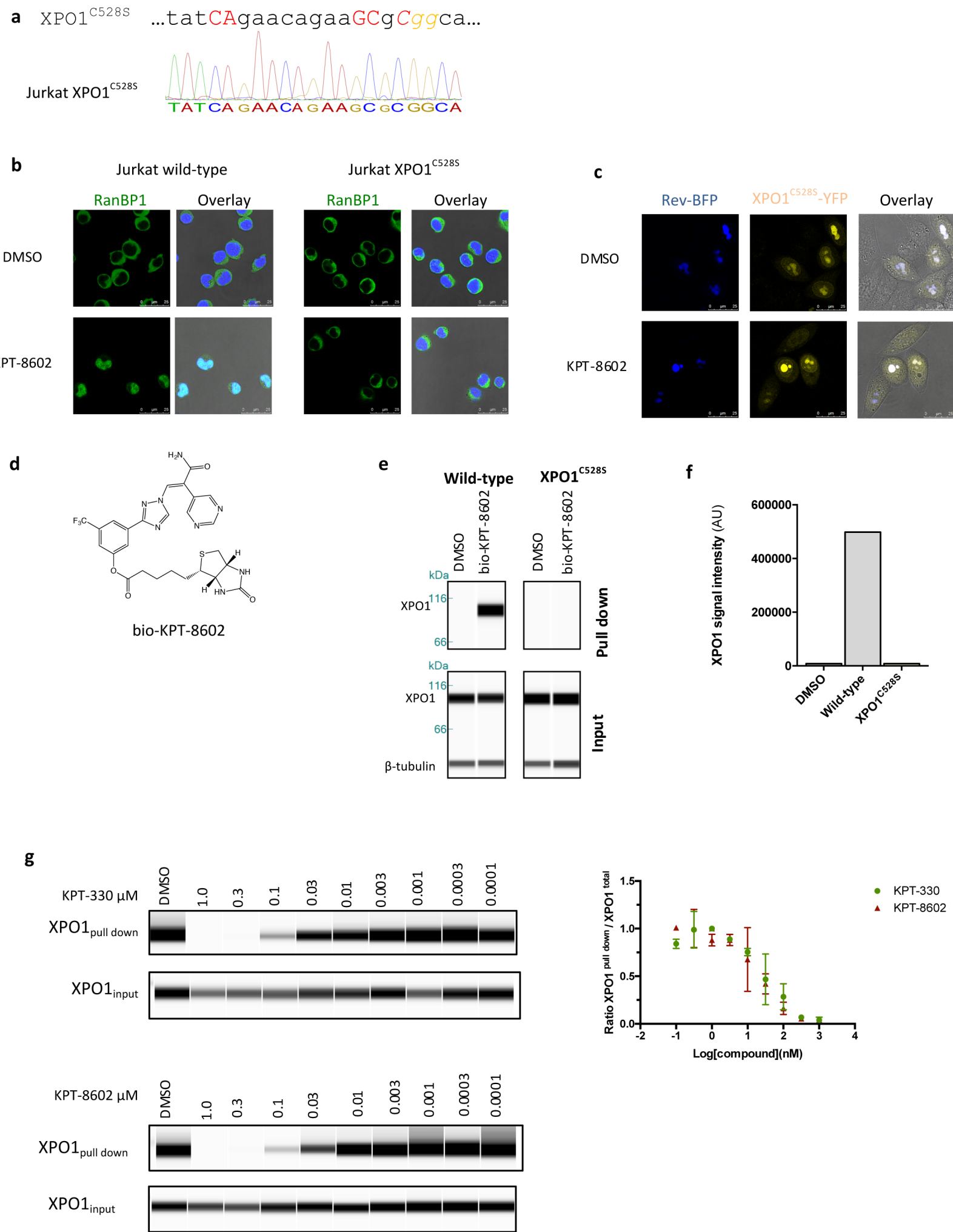
a
XPO1C528S
...tatCAgaacagaaGCgCggca...
Jurkat XPO1C528S
TATCAGAACAGAAGCGCGGCA
b
Jurkat wild-type
Jurkat XPO1C528S
RanBP1
Overlay
RanBP1
Overlay
DMSO
KPT-8602
c
Rev-BFP
XPO1C528S-YFP
Overlay
DMSO
KPT-8602
d
bio-KPT-8602
e
Wild-type
XPO1C528S
DMSO
bio-KPT-8602
DMSO
bio-KPT-8602
kDa
XPO1
116
66
Pull down
kDa
116
XPO1
66
β-tubulin
Input
f
XPO1 signal intensity (AU)
600000
400000
200000
0
DMSO
Wild-type
XPO1C528S
g
KPT-330 µM
DMSO
1.0
0.3
0.1
0.03
0.01
0.003
0.001
0.0003
0.0001
XPO1pull down
XPO1input
KPT-8602 µM
DMSO
1.0
0.3
0.1
0.03
0.01
0.003
0.001
0.0003
0.0001
XPO1pull down
XPO1input
Ratio XPO1 pull down / XPO1 total
1.5
1.0
0.5
0.0
-2
-1
0
1
2
3
4
Log[compound](nM)
KPT-330
KPT-8602

FIGURE 3

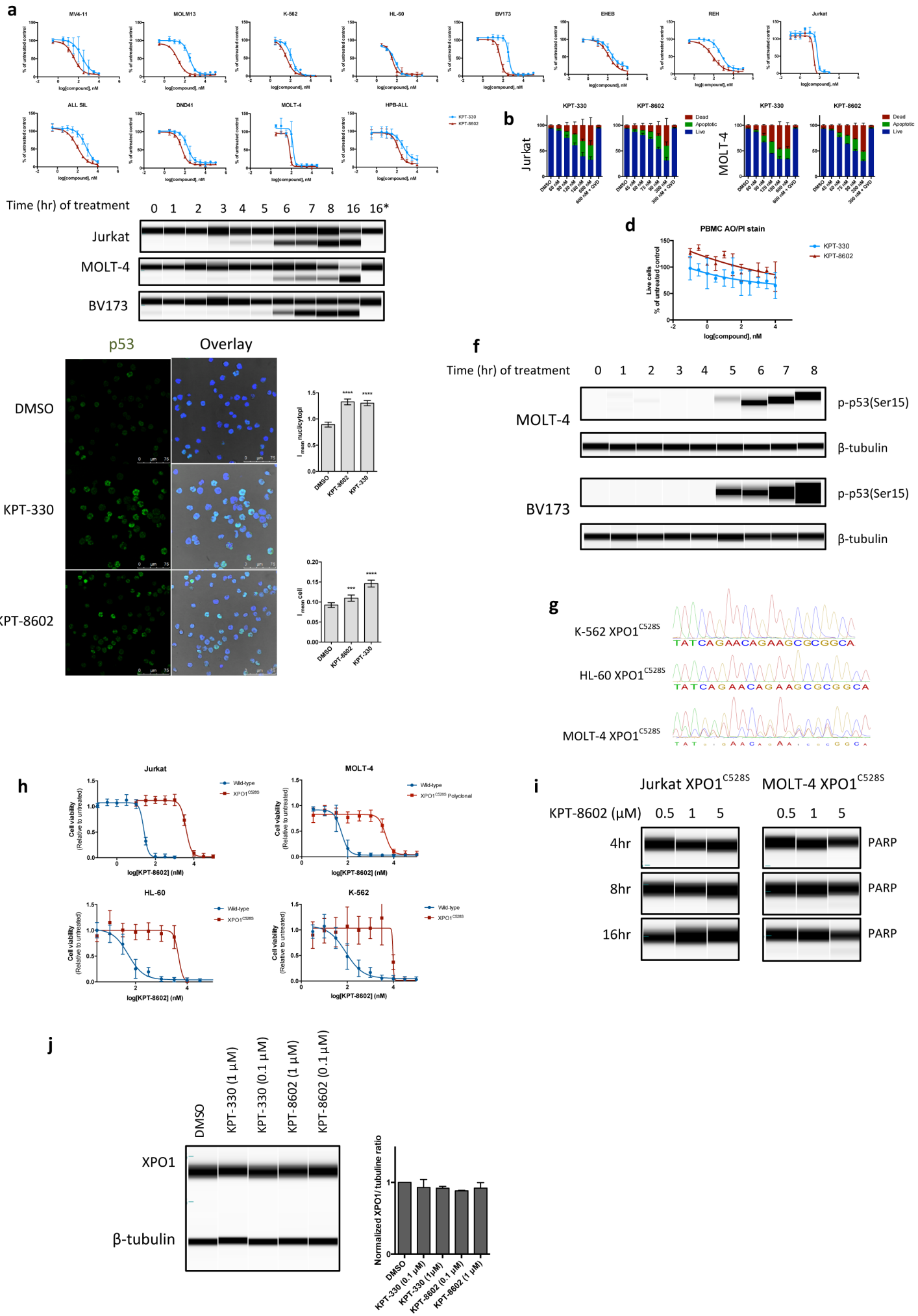
a
MV4-11
MOLM13
K-562
HL-60
BV173
EHEB
REH
Jurkat
ALL SIL
DND41
MOLT-4
HPB-ALL
% of untreated control
log[compound], nM
KPT-330
KPT-8602
b
KPT-330
KPT-8602
Jurkat
MOLT-4
Dead
Apoptotic
Live
c
Time (hr) of treatment
0 1 2 3 4 5 6 7 8 16 16*
Jurkat
MOLT-4
BV173
d
PBMC AO/PI stain
Live cells
% of untreated control
log[compound], nM
KPT-330
KPT-8602
e
p53
Overlay
DMSO
KPT-330
KPT-8602
DMSO
KPT-8602
KPT-330
f
Time (hr) of treatment
0 1 2 3 4 5 6 7 8
MOLT-4
BV173
p-p53(Ser15)
β-tubulin
g
K-562 XPO1C528S
HL-60 XPO1C528S
MOLT-4 XPO1C528S
TATCAGAACAGAAGCGCGGCA
h
Jurkat
MOLT-4
HL-60
K-562
Wild-type
XPO1C528S
XPO1C528S Polyclonal
Cell viability
(Relative to untreated)
log[KPT-8602] (nM)
i
Jurkat XPO1C528S
MOLT-4 XPO1C528S
KPT-8602 (μM) 0.5 1 5
0.5 1 5
4hr
8hr
16hr
PARP
j
DMSO
KPT-330 (1 μM)
KPT-330 (0.1 μM)
KPT-8602 (1 μM)
KPT-8602 (0.1 μM)
XPO1
β-tubulin
Normalized XPO1/ tubuline ratio

FIGURE 4

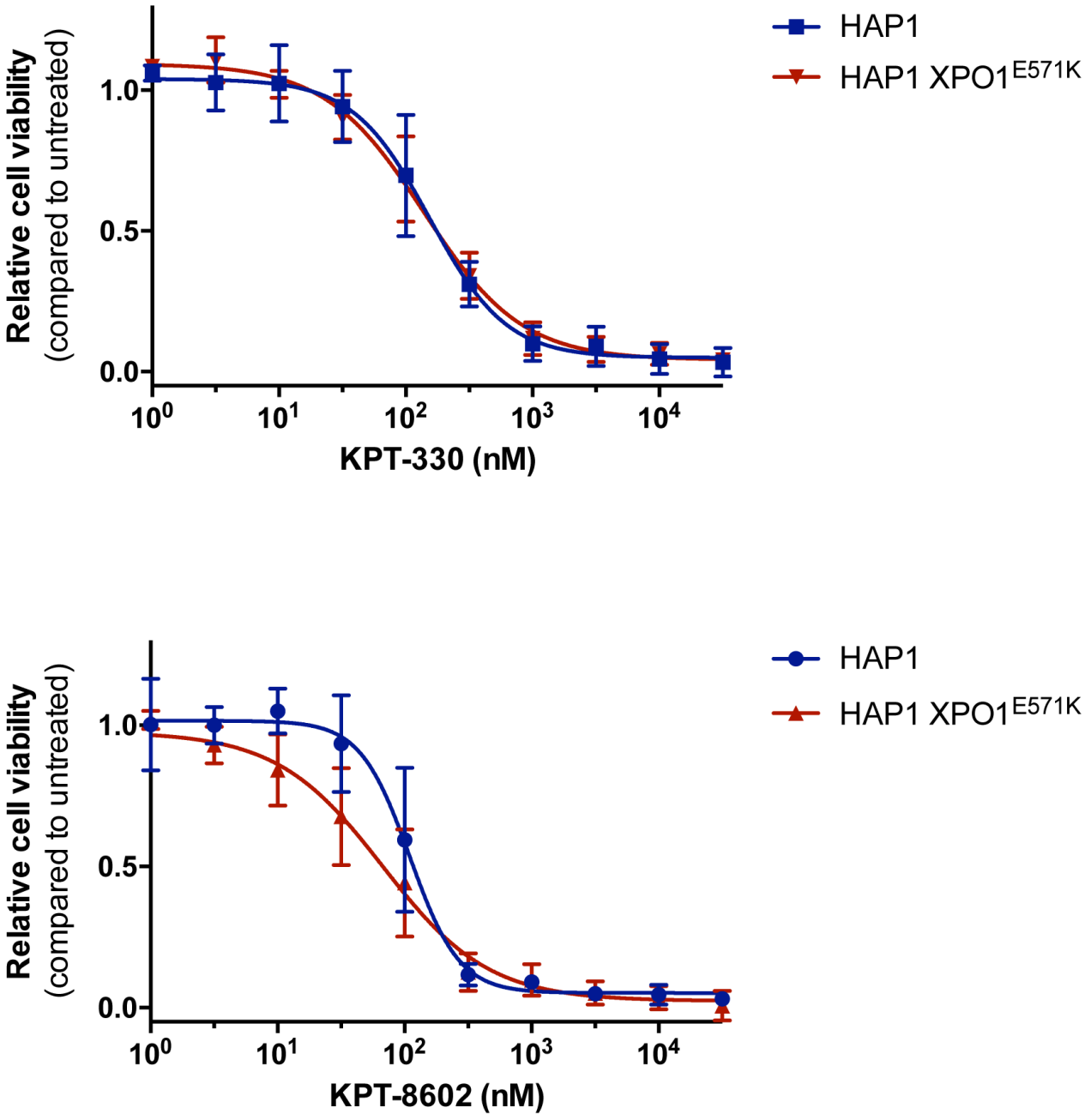
Relative cell viability
(compared to untreated)
1.0
0.5
0.0
10^0
10^1
10^2
10^3
10^4
KPT-330 (nM)
HAP1
HAP1 XPO1^{E571K}
Relative cell viability
(compared to untreated)
1.0
0.5
0.0
10^0
10^1
10^2
10^3
10^4
KPT-8602 (nM)
HAP1
HAP1 XPO1^{E571K}

FIGURE 5

A MOLT4 xenografts

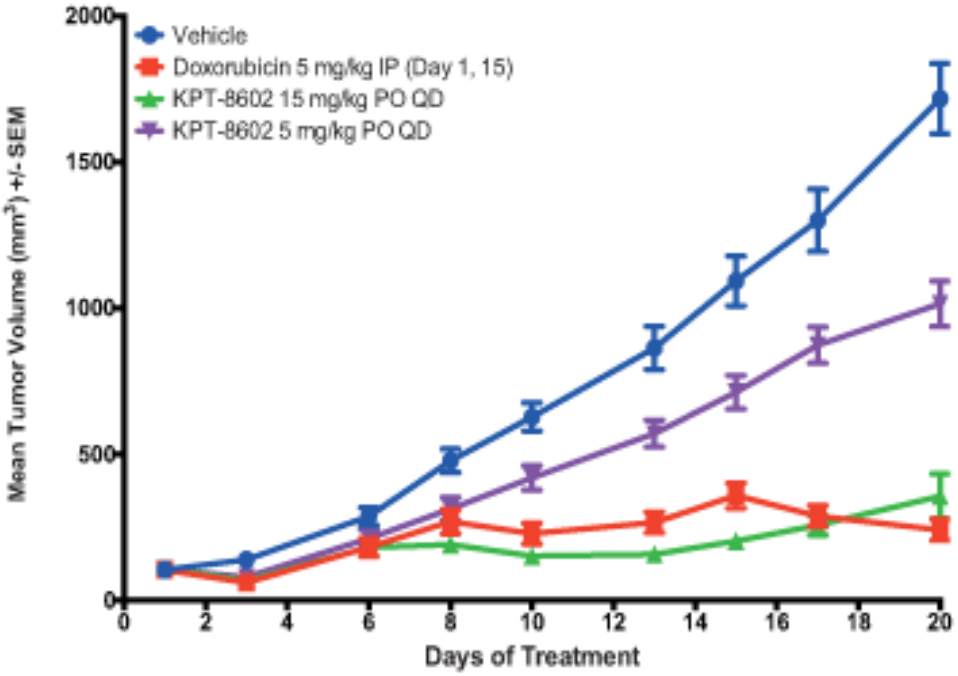

B JAK3(M511I) BALB/c-mice

C WILD-TYPE BALB/c-mice

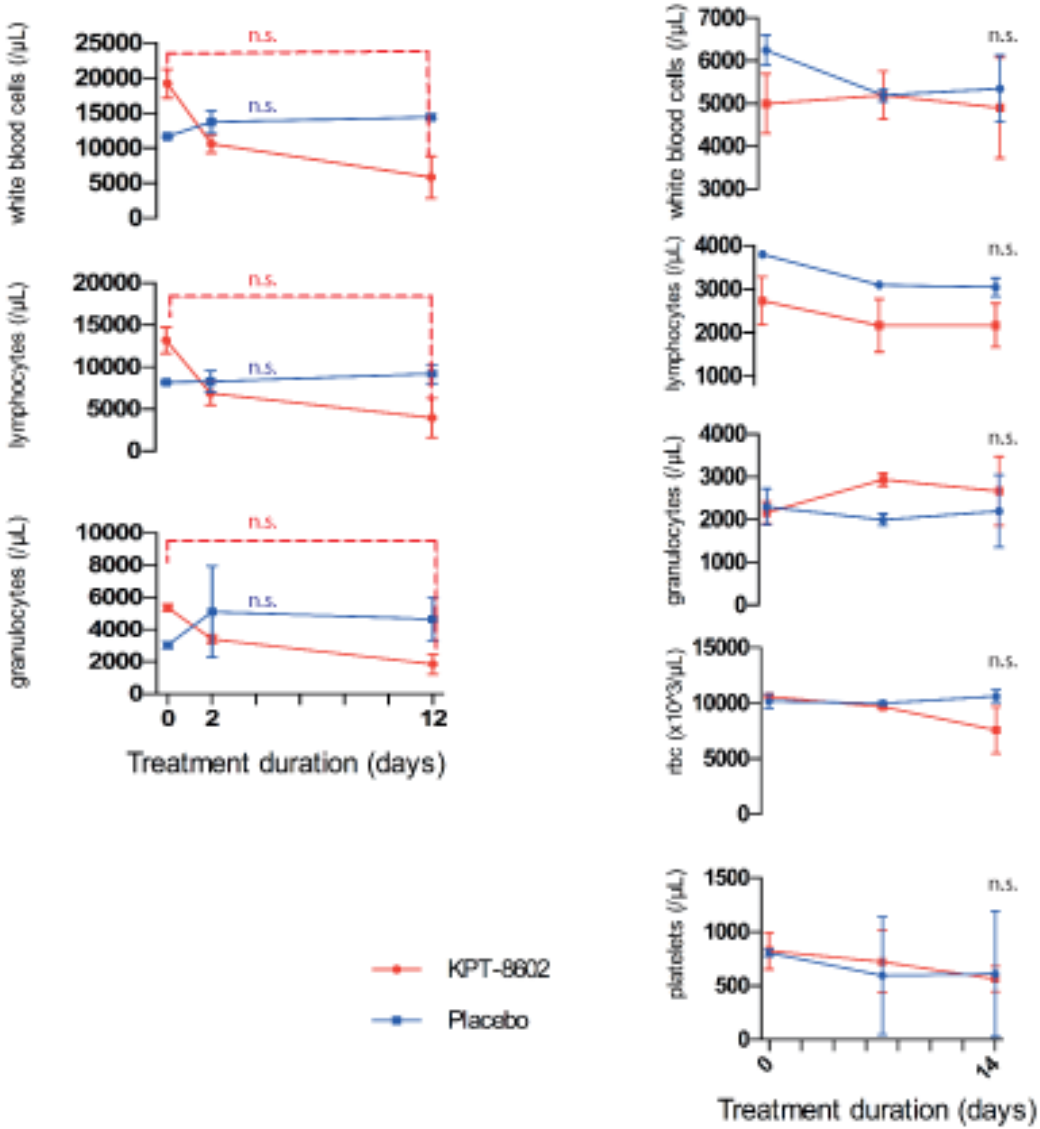

FIGURE 6

T-ALL PATIENT DERIVED XENOGRAFT MODEL

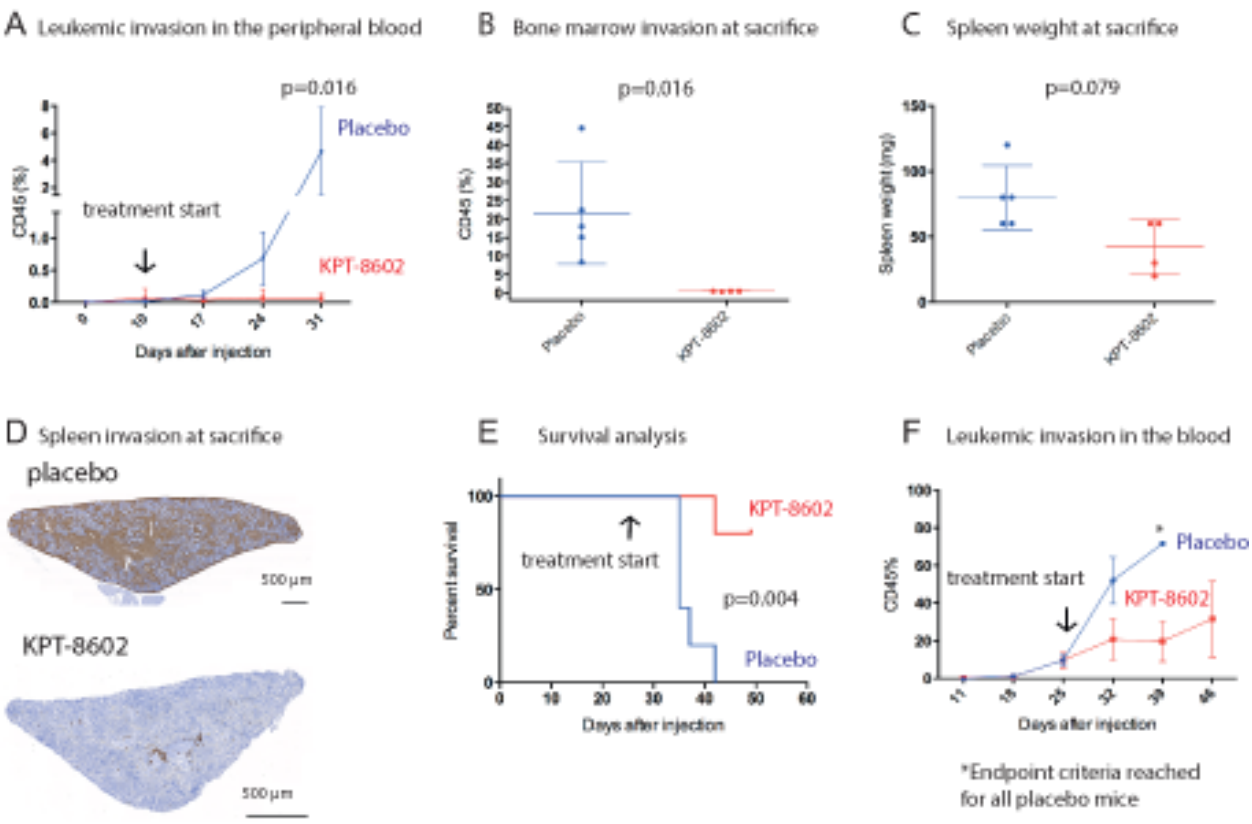

B-ALL PATIENT DERIVED XENOGRAFT MODEL